



## Effect of dimensionality on the charge-density wave in few-layer 2H-NbSe<sub>2</sub>

Matteo Calandra,<sup>1</sup> I. I. Mazin,<sup>2</sup> and Francesco Mauri<sup>1</sup>

<sup>1</sup>CNRS and Institut de Minéralogie et de Physique des Milieux Condensés, Case 115, 4 Place Jussieu, 75252, Paris Cedex 05, France

<sup>2</sup>Naval Research Laboratory, 4555 Overlook Avenue SW, Washington, DC 20375, USA

(Received 6 October 2009; revised manuscript received 30 November 2009; published 23 December 2009)

We investigate the charge-density wave (CDW) instability in single and double layers, as well as in the bulk 2H-NbSe<sub>2</sub>. We demonstrate that the density functional theory correctly describes the metallic CDW state in the bulk 2H-NbSe<sub>2</sub>. We predict that both monolayer and bilayer NbSe<sub>2</sub> undergo a CDW instability. However, while in the bulk the instability occurs at a momentum  $\mathbf{q}_{\text{CDW}} \approx \frac{2}{3}\Gamma M$ , in freestanding layers it occurs at  $\mathbf{q}_{\text{CDW}} \approx \frac{1}{2}\Gamma M$ . Furthermore, while in the bulk the CDW leads to a metallic state, in a monolayer the ground state becomes semimetallic, in agreement with recent experimental data. We elucidate the key role that an enhancement of the electron-phonon matrix element at  $\mathbf{q} \approx \mathbf{q}_{\text{CDW}}$  plays in forming the CDW ground state.

DOI: [10.1103/PhysRevB.80.241108](https://doi.org/10.1103/PhysRevB.80.241108)

PACS number(s): 71.45.Lr, 73.22.Lp, 74.25.Jb, 74.25.Kc

Charge-density wave (CDW) is one of the most common and most intriguing phenomena in solid-state physics.<sup>1</sup> The concept originated in the seminal paper of Peierls<sup>2</sup> pointing out a divergence in the one-dimensional (1D) response functions at a wave vector equal to twice the Fermi vector. Later this concept was generalized onto the two-dimensional (2D) and three-dimensional (3D) systems with “nesting,” that is, quasi-1D portions of the Fermi surface. On the other hand, the fact that the Peierls instability is logarithmic and therefore very fragile has led to the question of whether the actual CDWs observed in quasi-2D materials are indeed manifestations of the Peierls instability.<sup>3</sup>

In the past decades the role of nesting in various structural and magnetic instabilities has been wildly debated, particularly with respect to the most venerable CDW materials, NbSe<sub>2</sub>, and related dichalcogenides. It has been pointed out that the bare susceptibility does not have any sharp peak at the CDW wave vector,  $\mathbf{q}_{\text{CDW}} = (2\pi/3, 2\pi/3)$ , but at best a broad and shallow peak<sup>3-5</sup> in the real part, while the imaginary part [which directly reflects the Fermi surface (FS) nesting] does not peak at  $\mathbf{q}_{\text{CDW}}$  at all.<sup>3,5,6</sup>

This suggests that momentum dependence of the electron-phonon interaction plays a crucial role in driving CDW instabilities.<sup>3,5,7</sup> An indirect confirmation comes from neutron<sup>8</sup> and x-ray scattering<sup>9</sup> phonon-dispersion data where a marked softening was detected in only one of the low energy modes close to  $\mathbf{q}_{\text{CDW}}$ .

A very clean test for the described hypothesis would be to compare the bulk compound with purely 2D systems—monolayers and bilayers of the same composition. Lacking  $k_z$  dispersion, they should be much more sensitive to the Fermi surface nesting than their 3D counterparts. 2H-NbSe<sub>2</sub> is particularly promising as its 2D structures have been synthesized and found to show a curious semimetallic behavior.<sup>10</sup> Interestingly, the conductivity of a NbSe<sub>2</sub> layer in a field-effect transistor as a function of the gate voltage ( $V_g$ ), which controls the doping, is very different from that of good metallic monolayers. While typical metals have a conductivity rather weakly dependent on doping, NbSe<sub>2</sub> monolayers show a strong monotonic dependence on  $V_g$ . Such a large variation (more than a factor of 2 in the  $-70$  to  $+70$  V  $V_g$  range) is characteristic of semiconductors, semimetals as graphene, or metals with a pseudogap at the Fermi level. The

first-principles calculations predict a good metal for a monolayer in the undistorted bulk structure,<sup>11</sup> in disagreement with experiments, which suggest a possibility of a semimetallic band structure.

In this Rapid Communication we study the CDW instability in the bulk 2H-NbSe<sub>2</sub>, in the bilayer, and in the monolayer NbSe<sub>2</sub> both by calculating the phonon spectra in the high-symmetry phase and by full structural optimization.<sup>12</sup> We find that all three studied structures are unstable against a CDW formation with, however, *different* patterns despite the extreme similarity of the Fermi surfaces. We then demonstrate that the crucial difference comes from the  $\mathbf{q}$ -dependent electron-phonon matrix elements rather than directly from the FS. Finally we show that the CDW distorted monolayer is semimetallic and the large variation of its conductivity as a function of  $V_g$  detected in experiments is a manifestation of the CDW.

We simulate a single layer or a bilayer, as usually, by introducing a thick vacuum layer (of the order of 10 Å). We then performed the geometrical optimization in one unit cell, without a CDW. We found that the distance between the Nb and Se planes barely changes: from 1.67 Å in the bulk to 1.69 Å in the bilayer (same in the monolayer). On the contrary, the Nb-Nb interplanar distance in the bilayer is significantly enlarged compared to the bulk (6.27 Å vs 6.78 Å).

The pseudopotential electronic structure of the NbSe<sub>2</sub> bilayers and monolayers is compared with that of the bulk NbSe<sub>2</sub> in Fig. 1 [linearized augmented plane-wave (LAPW) calculations yield very similar results]. For the bulk case, as known from previous calculations,<sup>5,15</sup> three bands cross the Fermi level ( $\epsilon_F$ ). One is the antibonding Se  $p_z$  band, which is highly dispersive along the  $z$  axis and does not cross  $\epsilon_F$  in the  $A$ - $L$ - $H$  plane. The other two are formed by Nb  $d$  states and are degenerate in the  $A$ - $L$ - $H$  plane in the scalar relativistic calculations (spin-orbit interaction removes the degeneracy). The degeneracy is lifted for other values of  $k_z$  (Ref. 5) by the interlayer interaction. As a result, while one of the FSs originated from Nb  $d$  bands is two dimensional, the other acquires considerable  $k_z$  dispersion, so that a model neglecting hopping between the layers does not apply.<sup>16</sup>

In a bilayer, the Se-Se interplanar interaction is reduced, while in the monolayer it is absent. As a result, the Se band sinks below the Fermi level, and only the Nb-derived Fermi

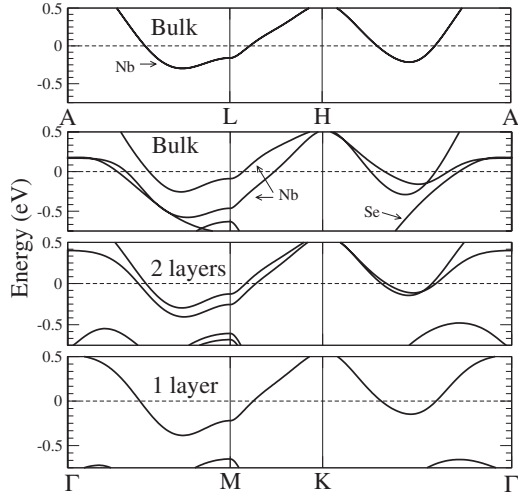


FIG. 1. Electronic structure of the undistorted bulk, bilayer, and monolayer 2H-NbSe<sub>2</sub>.

surfaces are present and they are strictly two dimensional, that is, seemingly more prone to the nesting effects. The calculated FS for a single layer (Fig. 2) consists of a rounded hexagon at  $\Gamma$  and two rounded triangles at  $K$ , just as the Nb FS pockets in the bulk 2H-NbSe<sub>2</sub>.<sup>5</sup>

Next, we have computed the phonon dispersions for the bulk and single-layer NbSe<sub>2</sub>. In Fig. 3 we plot the phonon dispersions in the monolayer (bulk) calculated using a  $40 \times 40$  ( $20 \times 20 \times 6$ )  $k$ -point grid and Fermi temperature  $\tau = 68$  meV ( $\tau = 270$  meV) with Hermite-Gaussian distributions (see Ref. 17 for more details). In the bulk, the highest energy acoustic mode is unstable at  $\mathbf{q}_{\text{CDW}} \approx 2/3\Gamma M$ , in agreement with the experiment. These calculations implicitly include the renormalization of the bare phonon frequencies due to the electron-phonon interaction, as described by the real part of the phonon self-energy of a phonon mode  $\mu$ , namely,

$$\Pi'_{\tau,\mu}(\mathbf{q}, \omega=0) \sim \sum_{\mathbf{k}, nm} \frac{|g_{\mathbf{k}i, \mathbf{k}+\mathbf{q}, j}^{\tau, \mu}|^2 (f_{\mathbf{k}+\mathbf{q}, j}^{\tau} - f_{\mathbf{k}i}^{\tau})}{\epsilon_{\mathbf{k}+\mathbf{q}, j}^{\tau} - \epsilon_{\mathbf{k}, i}^{\tau}}, \quad (1)$$

where  $\epsilon_{\mathbf{k}i}$  is the one-electron energy,  $g_{\mathbf{k}i, \mathbf{k}+\mathbf{q}, j}^{\mu}$  is the electron-phonon matrix element, and  $f_{\mathbf{k}i}^{\tau}$  is the Fermi function. If one neglects the  $\mathbf{k}$  dependence of the matrix elements in Eq. (1), this expression becomes proportional to the real part of the unrenormalized static electronic susceptibility,  $\chi'_0(\mathbf{q})$ ; as

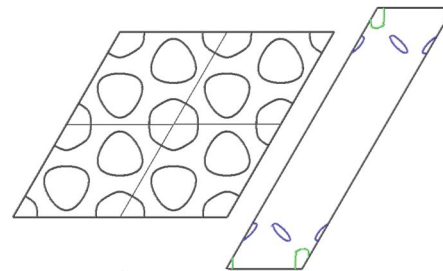
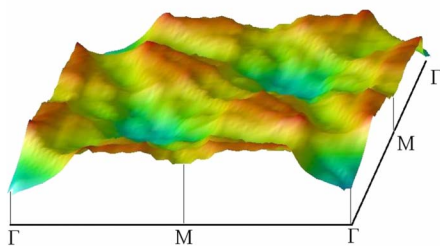


FIG. 2. (Color online) Left: real part of the bare static electronic susceptibility (in arbitrary units) with constant matrix elements, same as the real part of the phonon self-energy  $\Pi'_{\sigma,\mu}(\mathbf{q}, \omega=0)$  [Eq. (1)], calculated using the LAPW band structure of a single layer NbSe<sub>2</sub>. Center: the corresponding FS. Four Brillouin zones are shown;  $\Gamma$  points are at the grid nodes. Right: the same for the resulting  $4 \times 1$  CDW.

shown in Ref. 5, in NbSe<sub>2</sub>  $\chi'_0(\mathbf{q})$  has a broad maximum at  $\mathbf{q}_{\text{CDW}} = 2/3\Gamma M$ , even though the imaginary part (which directly reflects the FS nesting) does not.

Thus, density functional theory (DFT) correctly describes the CDW instability in the bulk NbSe<sub>2</sub>. With this in mind, we move to a NbSe<sub>2</sub> monolayer and observe that (a) now the most unstable phonon mode along  $\Gamma M$  appears near  $(1/2)\Gamma M = (0.5\pi/a, 0)$  and (b) the instability expands over a substantially larger  $k$ -point region as phonons are unstable also along  $MK$ . We also looked at the bare susceptibility  $\chi'_0$  and found a striplike region of enhanced values, extending from  $0.4\Gamma M$  to  $0.75\Gamma M$ , with a width of approximately 0.15 of the  $\Gamma M$  vector ( $0.15\pi/a$ ). This is in agreement with the instabilities found in the linear-response phonon calculations along  $\Gamma M$  and  $MK$ .

To understand which electronic states are involved in the CDW formation we have repeated the calculations with an increased electronic temperature  $\tau$ . We found that the phonon frequency of the highest acoustic mode strongly depends on  $\tau$  for  $\tau > 0.3$  eV. The instability occurs for  $\tau \approx 0.3$  eV, and for smaller temperatures the (imaginary) phonon frequency of the unstable mode is essentially constant. This means that electronic states within a 0.3 eV window around  $\epsilon_F$  are responsible for the CDW instability, which is not a Fermi surface effect<sup>4,18–20</sup> but involves states in the full Nb-derived  $d$  band [which is only 1 eV wide (see Fig. 4)]. As discussed above,  $\chi'_0$  does have a maximum at  $\mathbf{q}_{\text{CDW}}$ , but this maximum is relatively weak and broad, and, most importantly, weakly dependent on  $\tau$ . Thus, the CDW is mainly the result of an enhancement of the electron-phonon matrix element close to  $\mathbf{q}_{\text{CDW}}$ . The self-consistent screening of the electron-phonon matrix element as a function of  $\tau$  is crucial to describe the CDW.

The next test is to take a superstructure suggested by the calculated CDW vector [ $(\pi/3, 0)$  or  $(\pi/4, 0)$ ] and to optimize the cell dimensions and the atomic positions. Each time we started from slightly randomized atomic positions and minimized the total energy. We found that in the bulk the  $4 \times 1$  and  $3 \times 1$  supercells both converge to a lower energy than the undistorted cell, consistent with the calculated phonon spectra in Fig. 3, the  $3 \times 1$  being lower in energy (with the energy gain of 0.1 mRy/Nb with respect to the undistorted structure). The other supercells converged to the undistorted structure. The distortion of the  $3 \times 1$  supercell is consistent with the  $\Sigma_1$  phonon pattern detected in inelastic neutron scattering,<sup>8</sup> involving not only an in-plane deforma-

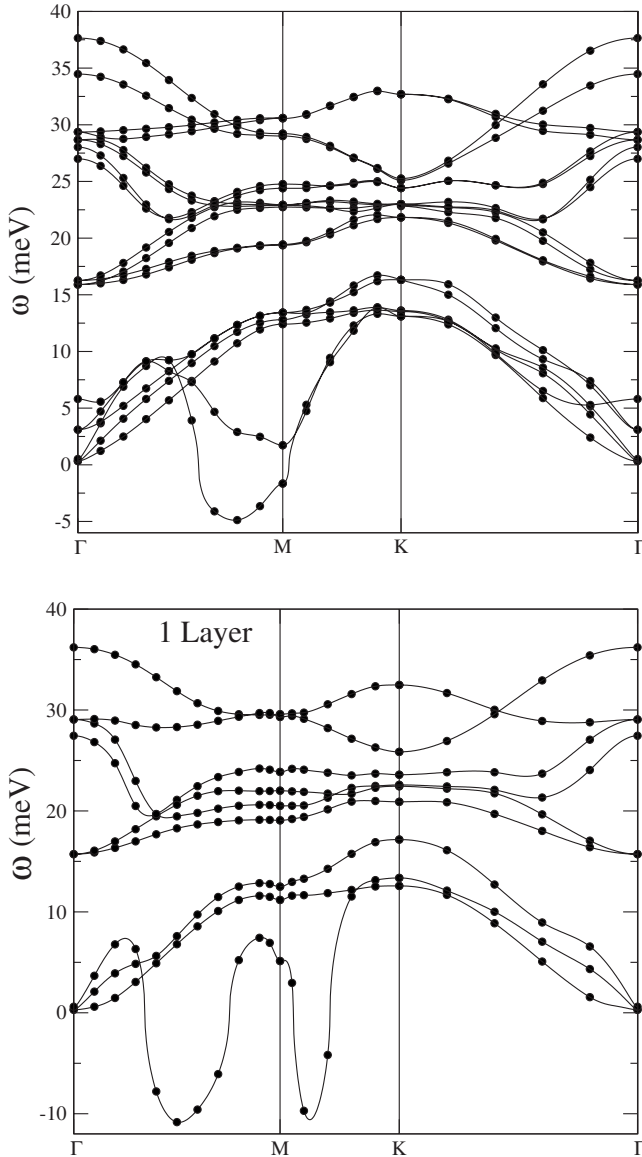


FIG. 3. Phonon dispersion of bulk (top) and monolayer (bottom) 2H-NbSe<sub>2</sub>. Each point corresponds to a linear-response calculations. The spline connecting the points is guide for the eyes.

tion of the layered structure but also out-of-plane displacements of the Se atoms and a charge transfer between the two layers.

For a monolayer, the situation is different. The lowest energy supercell is now  $4 \times 1$  with a 1.19 mRy/Nb energy gain with respect to the undistorted cell, followed by  $3 \times 1$ . We also checked the  $2 \times 1$  and  $2 \times 2$  supercells, which converged to the undistorted structure, and the  $3 \times 3$  one, which converged to the same structure as  $3 \times 1$ . This is again consistent with the calculated phonon spectra. In the ground state Nb atoms are trimerized, qualitatively different from the bulk CDW. Finally, the bilayer behaves just like a monolayer, with a  $4 \times 1$  ground state similar to that found for a monolayer.

Having obtained the distorted structure both for the bulk and for a monolayer, we investigated their electronic properties. We found (Fig. 4) that in the bulk case the density of states (DOS) at the Fermi level in the distorted  $3 \times 1$  super-

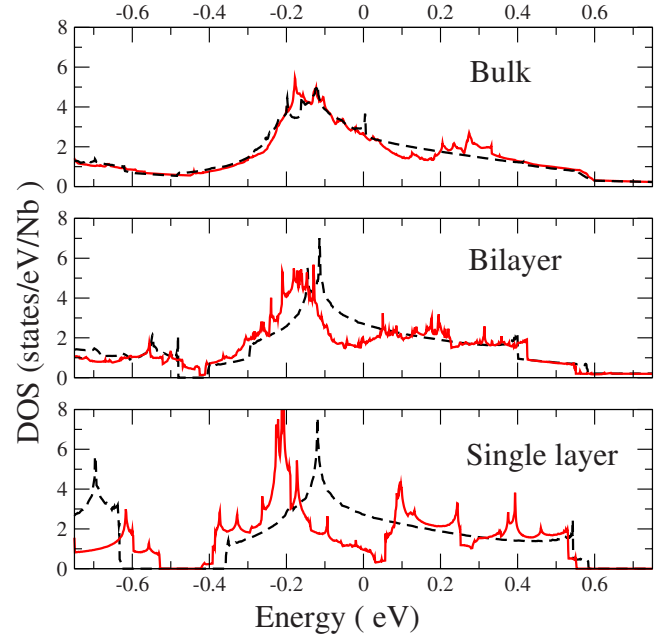


FIG. 4. (Color online) Pseudopotential electronic density of states for undistorted (black dashed) and distorted (red) bulk, bilayer, and monolayer 2H-NbSe<sub>2</sub>.

cell is not much reduced in the CDW, contrary to what one would expect in the Peierls model, and reconfirming that the energy gain in this case is not coming from the states in the immediate vicinity of the Fermi level<sup>5</sup> but from the occupied Nb bands. In the monolayer  $4 \times 1$  supercell the Peierls model is again violated due to the important role of the electron-phonon matrix element, however the FS is strongly gapped (see Fig. 2, right) and displays a clear semimetallic behavior in qualitative agreement with experimental data.<sup>10</sup>

More insight on the conducting nature of the monolayer is obtained from the conductivity per layer, namely,

$$\sigma_x^{2D}(E) = \frac{e^2}{3\Omega_{2D}N_k} \sum_{\mathbf{k}i} v_{\mathbf{k}i,x}^2 \tau(\mathbf{k}) \delta(\epsilon_{\mathbf{k}i} - E), \quad (2)$$

where  $\Omega_{2D}$  is the area of the two-dimensional unit cell of a NbSe<sub>2</sub> layer,  $e$  is the electron charge,  $N_k$  is the number of  $k$  points used in the calculation,  $\mathbf{v}_{\mathbf{k}i}$  is the electron velocity, and  $E$  is the energy. In general  $\sigma_x^{2D}(E) = \sigma_x^{3D}(E) \times L$ , where  $L = 6.275 \text{ \AA}$  is the layer thickness. Assuming  $\tau(\mathbf{k}) \approx \tau(\epsilon_F)$ , we have that  $\sigma_{ab}^{2D}(E) = L\tau(\epsilon_F)\omega_{p,ab}^2/4\pi$ .

The  $\omega_{p,ab}^2$ , calculated using the *optics* code of the WIEN2K package, are plotted in Fig. 5 for the monolayer NbSe<sub>2</sub> as a function of the gate-induced charge as obtained from the DOS (Fig. 4). For the undistorted structures,  $\omega_{p,ab}$  is almost constant, in disagreement with the experiment. On the contrary, in the CDW state the monolayer plasma frequency shows substantial variation near  $\epsilon_F$  due of its semimetallic structure. A pseudogap occurs just above  $\epsilon_F$ , so that the conductivity grows with the gate voltage. In the constant relaxation-time approximation and assuming an electron self-doping of  $\approx 30 \times 10^{12} \text{ cm}^{-2}$  we obtain reasonable agreement with experimental conductivity as a function of the gate voltage<sup>10</sup> (see Fig. 5). For a quantitative comparison with

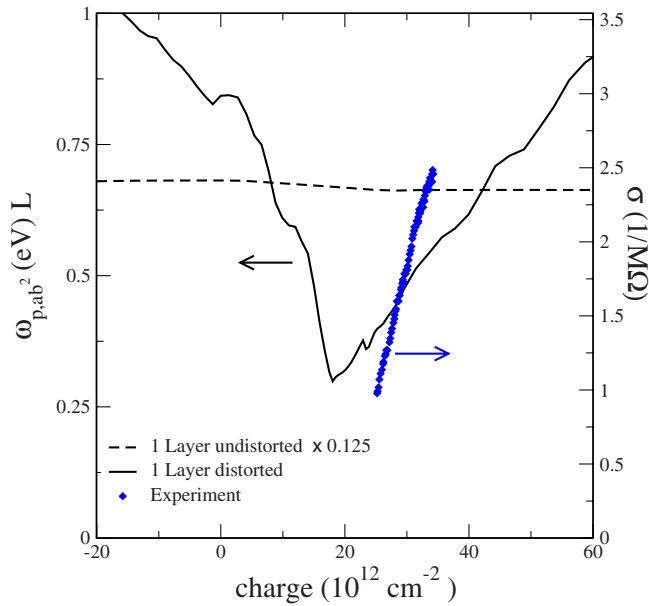


FIG. 5. (Color online) LAPW plasma frequency and conductivity as a function of the gate-induced charge for a single-layer NbSe<sub>2</sub>. The constant relaxation-time approximation is adopted. Experimental data (Ref. 10) are plotted assuming the charge neutrality at  $\approx 30 \times 10^{12} \text{ cm}^{-2}$ . The gate voltage for the standard configuration of a 300 nm SiO<sub>2</sub> field-effect transistor can be obtained from the  $x$  axis divided by  $7.2 \times 10^{-2} \text{ cm}^{-2} \text{ V}^{-1}$ . The charge is obtained from the integrated DOS.

experiments, however, one would need to know the energy and momentum dependence of  $\tau$ .

To summarize, we have shown that DFT accurately describes the CDW instability in the bulk 2H-NbSe<sub>2</sub> and predicts a similar instability to occur in monolayer and bilayer. However, while in the bulk the CDW occurs at  $\mathbf{q}_{\text{CDW}} \approx (\frac{1}{3}, 0, 0) \frac{2\pi}{a}$ , in the monolayer and bilayer the CDW vector is  $\approx (\frac{1}{4}, 0) \frac{2\pi}{a}$ , in agreement with what was found in Ref. 23 for the case of TaSe<sub>2</sub>. In all these systems the CDW is driven by an enhancement of the electron-phonon coupling at  $\mathbf{q} \sim \mathbf{q}_{\text{CDW}}$ . Our work solves the long-standing controversy on the origin of CDW in 2H-NbSe<sub>2</sub> and in transition-metal dichalcogenides.

Unlike the bulk case, when the system remains a good metal in the CDW state, in a monolayer CDW produces a semimetallic state. For a charge of  $30 \times 10^{12} \text{ cm}^{-2}$  in Fig. 5, we have that the ratio of the experimental conductivity per layer is  $\sigma_{ab}^{2D, \text{bulk}} / \sigma_{ab}^{2D, 1 \text{ layer}} = \omega_{p,ab, \text{bulk}}^2 \tau^{\text{bulk}} / (\omega_{p,ab, 1 \text{ layer}}^2 \tau^{\text{1 layer}}) = 243$ . This is due to a reduction of the plasma frequency of a factor 12.4 and to a suppression of the relaxation time of a factor 19.6 in going from the bulk to the monolayer.

The semimetallic behavior of the monolayer leads to a large variations of the conductivity as a function of the gate voltage, contrary to the undistorted structure and in agreement with the experiment.<sup>10</sup> Our calculation shows that a proper description of the CDW instability in reduced dimension is mandatory to interpret conduction data for low-dimensional transition-metal dichalcogenides and opens the way to theoretical understanding of CDW-based field-effect devices.

Calculations were performed at the IDRIS Supercomputing Center (Project No. 081202).

<sup>1</sup>G. Grüner, *Density Waves in Solids* (Addison-Wesley, Reading, PA, 1994).

<sup>2</sup>R. E. Peierls, *Quantum Theory of Solids* (Clarendon, Oxford, 1955).

<sup>3</sup>M. D. Johannes and I. I. Mazin, Phys. Rev. B **77**, 165135 (2008).

<sup>4</sup>N. J. Doran, B. Ricco, M. Schreiber, D. Titterton, and G. Wexler, J. Phys. C **11**, 699 (1978).

<sup>5</sup>M. D. Johannes, I. I. Mazin, and C. A. Howells, Phys. Rev. B **73**, 205102 (2006).

<sup>6</sup>M. H. Whangbo and E. Canadell, J. Am. Chem. Soc. **114**, 9587 (1992).

<sup>7</sup>N. J. Doran, J. Phys. C **11**, L959 (1978).

<sup>8</sup>D. E. Moncton, J. D. Axe, and F. J. Salvo, Phys. Rev. Lett. **34**, 734 (1975); Phys. Rev. B **16**, 801 (1977).

<sup>9</sup>B. M. Murphy, H. Requardt, J. Stettner, J. Serrano, M. Krisch, M. Müller, and W. Press, Phys. Rev. Lett. **95**, 256104 (2005); J. Phys.: Condens. Matter **20**, 224001 (2008).

<sup>10</sup>K. S. Novoselov *et al.*, Proc. Natl. Acad. Sci. U.S.A. **102**, 10451 (2005).

<sup>11</sup>S. Lebègue and O. Eriksson, Phys. Rev. B **79**, 115409 (2009).

<sup>12</sup>Calculations were performed using the QUANTUM-ESPRESSO (Ref. 13) pseudopotential code and the WIEN2K (Ref. 14) all-electron

LAPW package with the generalized gradient approximation. For Nb (Se) we use ultrasoft (Ref. 21) [norm-conserving (Ref. 22)] pseudopotentials including semicore states as valence.

<sup>13</sup>P. Giannozzi *et al.*, J. Phys.: Condens. Matter **21**, 395502 (2009), <http://www.quantum-espresso.org>

<sup>14</sup>P. Blaha, K. Schwarz, G. K. H. Madsen, D. Kvasnicka, and J. Luitz, *WIEN2K: An Augmented Plane Wave+Local Orbitals Program for Calculating Crystal Properties* (Technische Universität Wien, Vienna, 2001).

<sup>15</sup>L. F. Mattheiss, Phys. Rev. Lett. **30**, 784 (1973); Phys. Rev. B **8**, 3719 (1973).

<sup>16</sup>D. S. Inosov *et al.*, New J. Phys. **10**, 125027 (2008).

<sup>17</sup>M. Calandra and F. Mauri, Phys. Rev. Lett. **95**, 237002 (2005).

<sup>18</sup>T. M. Rice and G. K. Scott, Phys. Rev. Lett. **35**, 120 (1975).

<sup>19</sup>J. A. Wilson, Phys. Rev. B **15**, 5748 (1977).

<sup>20</sup>Th. Straub, T. Finteis, R. Claessen, P. Steiner, S. Hufner, P. Blaha, C. S. Oglesby, and E. Bucher, Phys. Rev. Lett. **82**, 4504 (1999).

<sup>21</sup>D. Vanderbilt, Phys. Rev. B **41**, 7892 (1990).

<sup>22</sup>N. Troullier and J. L. Martins, Phys. Rev. B **43**, 1993 (1991).

<sup>23</sup>G. Benedek, G. Brusdeylins, C. Heimlich, L. Miglio, J. G. Sko-ronick, J. P. Toennies, and R. Vollmer, Phys. Rev. Lett. **60**, 1037 (1988).